JOURNAL OF AIRCRAFT
Vol. 31, No. 3, May–June 1994

Loading Characteristics of Finite Wings Undergoing Rapid Unsteady Motions: A Theoretical Treatment

Eric J. Jumper* and Ronald J. Hugo†
University of Notre Dame, Notre Dame, Indiana 46556

This article describes an unsteady, incompressible, lifting-line method for determining spanwise loading and moments on a wing undergoing arbitrary dynamic motions. The method is compared to an unsteady vortex-lattice method and a constant-source, constant-doublet paneling method and appears to predict span loading as well as these methods. The method is also compared to experimental data for an aspect-ratio-four wing undergoing a near-constant pitch-rate motion.

I. Introduction

IN steady aerodynamics it is well known that the loading on a finite wing (three-dimensional) differs substantially from that of an airfoil/wing section (two-dimensional). In the absence of viscosity and compressibility, these differences are primarily attributable to downwash effects due to the streamwise free vortices associated with the spanwise bound, circulation-strength distribution giving rise to the lift of the wing.[1] As such, reports that the spanwise loading of a wing undergoing a rapid pitching motion is more two-dimensional-like than three-dimensional-like, as reported by Robinson, Wissler, and Walker (RWW) (Ref. 2) is of interest to the applied aerodynamicist,[3] since advanced aircraft designs seek to exploit rapid rotation rates in an attempt to enhance "agility."[4] It is, therefore, important to develop a feel for why these phenomena occur and to develop methods that are both quick and easy enough for designers and analysts to use to predict unsteady loading in ways analogous to those in which steady two-dimensional results are extendable to finite-wing, spanwise loading.

These sentiments are nearly identical to those expressed by Bisplinghoff et al.[5] when addressing the need for general unsteady wing-loading methods for applications to aeroelasticity, as they state, "even ones having a scope comparable with the subsonic lifting-line equation." Their 1955 comments acknowledged the increasing availability of "high-speed digital computing machines" so that, in encouraging the development of such a method, the number of numerical operations per solution could be large. The first documented effort to develop an unsteady lifting-line method was that by Cicala[6] in 1938, for an elliptic-planform, oscillating wing, and this method was later extended to a swept, symmetrically loaded, oscillating wing by Dengler and Goland.[7] Other, independent methods have also been developed[8]; however, as pointed out by Fung,[8] the problem was perceived to be so complicated that even after linearization no practical exact solution was thought to exist, even for very restricted loading and motion constraints. Furthermore, Fung pointed out that independent approaches to approximate solutions could not be shown to be equivalent. Since 1955 there have only been a few attempts at developing an unsteady lifting-line method; one example is that by Beddoes[9] which involves concepts similar to those presented here, but takes a different approach.

For the most part, with the increasing availability of computers, the direction in wing theory (steady and unsteady) drifted away from theoretical solutions (like lifting-line methods) and toward what are now referred to as lifting surface and paneling methods. Yet, with the general availability of three-dimensional paneling methods and very high-speed workstation computers, unsteady paneling methods are still limited in their range of dynamic motions (cf., below) due primarily to run-time limitations. Also, it is difficult to assess the accuracy of the various unsteady paneling-method predictions for the same reasons mentioned by Bisplinghoff et al.[5] for assessing the merits of approximate methods, i.e., in their words, a "paucity of experimental data." This situation has little improved since 1955, which may explain why the data from experiments on rapidly pitching wings, like those of Ref. 2, appear surprising.

With regard to developing a feel for why spanwise, unsteady wing loading during rapid wing motions behaves differently from steady wing loading, in a previous paper[10] we presented a simple model (Fig. 1) that considered a uniform bound vortex of strength Γ connected by two streamwise, wingtip vortices to a spanwise, uniform, free starting vortex. The starting vortex was allowed to convect at the freestream velocity V_∞.

The resulting spanwise downwash distribution was computed at various times and normalized by the downwash due to a two-dimensional starting shed-vortex.[10] By ratioing the solutions, we were able to estimate the times and span locations over which unsteady three-dimensional solutions might look somewhat two-dimensional. Figure 2 gives an example of where the ratio of the center-span downwash to span three-dimensional downwash vs span location y is given at various nondimensional times ($t^* = V_\infty t/b$, where t is the dimensional time, and b is the wing span). Figure 3 gives the two-dimensional unsteady downwash ratioed to the three-dimensional unsteady downwash at the center span.

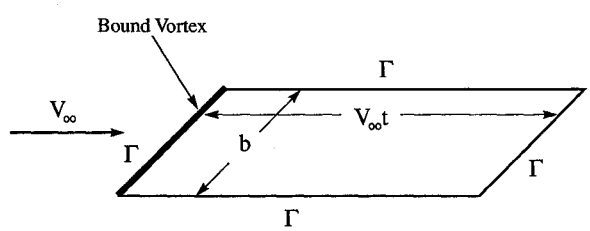

Fig. 1 Vortex system for simple model.

Presented as Paper 91-3263 at the AIAA 9th Applied Aerodynamics Conference, Baltimore, MD, Sept. 23–25, 1991; received Feb. 11, 1992; revision received Feb. 12, 1993; accepted for publication Feb. 15, 1993.

*Associate Professor, Department of Aerospace and Mechanical Engineering. Associate Fellow AIAA.
†Graduate Assistant, Department of Aerospace and Mechanical Engineering. Member AIAA.

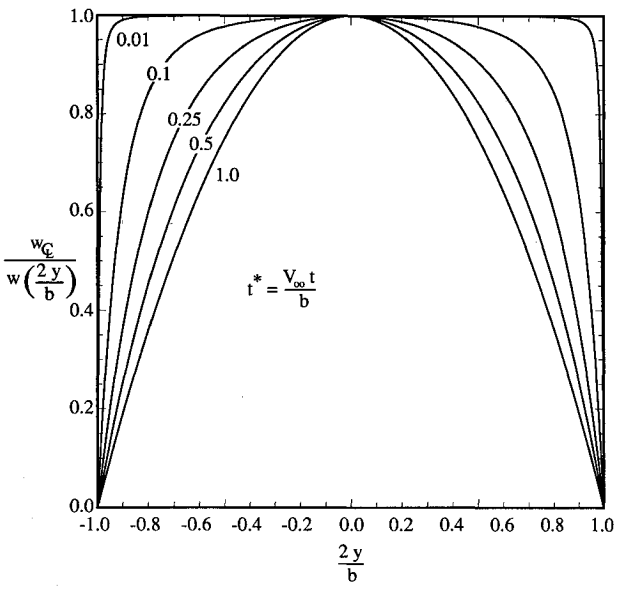

Fig. 2 Downwash distribution as a function of nondimensional time.

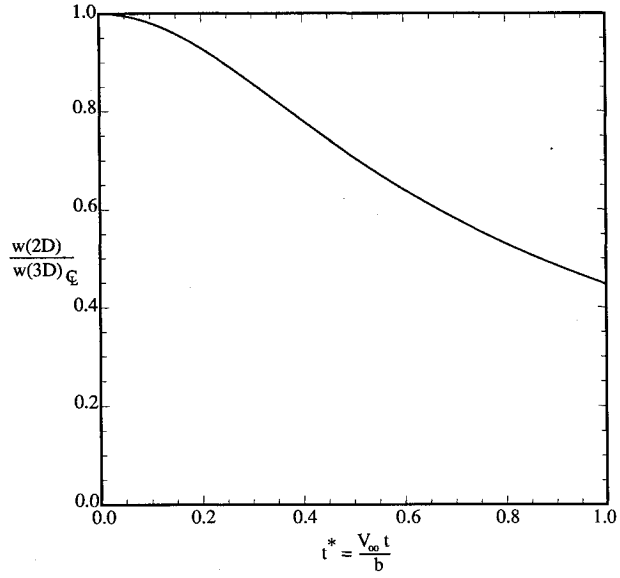

Fig. 3 Two-dimensional unsteady downwash relative to that at the centerline of a three-dimensional wing.

While this model gives a feel for why three-dimensional loading might mimic two-dimensional loading for a short time, it is not useful in attempting to predict unsteady loading for a variety of reasons, not the least of which is that the simple model included no mechanism for allowing the wake vortices to interact and modify the bound-circulation strength. In considering the limitations of that simple model, we were led to the realization that with the work we were performing in the area of two-dimensional unsteady aerodynamics (cf., below), an unsteady, nonrestrictive, and quick lifting-line method was possible.

This article presents our unsteady, incompressible, lifting-line method and addresses its validity. Among other comparisons, the method is applied to the RWW experimental data[2] which serves as both a further validation and an explanation of some of the physics involved in the experiment.

II. Steady Lifting-Line Theory

The classic Prandtl model for a wing in steady unseparated flow is based on the so-called "lifting-line" representation.[1,7,11,12] The key assumption in this model is that the wing is replaced by a spanwise vortex filament of nonuniform strength $\Gamma(y)$. This spanwise filament is connected to uniform strength filaments (an infinite number in the limit) extending to infinity in the downstream direction; the strength of each filament is equal to the change in the spanwise vortex strength. At each span location, the wing section is replaced by the filament's vortex strength based on the wing-section's circulation if it were in a two-dimensional flow at an angle of attack equal to the geometric angle of the wing at that section, but modified by the "downwash angle," the downwash being induced by the streamwise vortices.[1,12] The lift per unit span L', at a given spanwise location y, is determined by using the Kutta-Joukowski theorem

$$L'(y) = \rho V_\infty \Gamma(y) \tag{1}$$

where ρ is the density. The spanwise vortex strength may be determined approximately for an arbitrary symmetrical wing loading by Fourier decomposing the vortex strength as described in Ref. 1. This method requires knowledge of the steady two-dimensional airfoil lift-curve slope.

From the point of view of extending lifting-line theory to unsteady flows, two things must be kept in mind. First, as pointed out by Dengler and Goland,[7] the wing is replaced by a line vortex immersed in a body of fluid, and, as such, the vortex has no chord length. In this regard, all wing-section effects (i.e., chord, camber, thickness, etc.) are derived from two-dimensional airfoil analysis. Second, in the steady case, the lift per unit span and the section circulation, i.e., the local vortex strength, are related through the Kutta-Joukowski theorem [Eq. (1)]. Unfortunately, no equivalent unsteady form of the Kutta-Joukowski theorem relating lift to circulation exists, since the time rate of change in vorticity distribution must be known rather than just the time rate of change in the circulation. This means that both the lift and the circulation must be related directly back to the unsteady two-dimensional airfoil analysis.

III. Unsteady Lifting-Line Theory

Keeping the underlying premises from steady lifting-line theory in mind, we extended the theory to unsteady flow by using equations developed for two-dimensional unsteady airfoil theory[13-15] to predict the section lift coefficient, moment coefficient, and circulation as functions of span location and time. Furthermore, as a check on validity, we required that the unsteady lifting-line theory asymptote to steady lifting-line theory should wing motion stop, and after sufficient time elapses.

A. Unsteady Lift Relation

In order to solve for the unsteady lift at any span location, one must first know the previous angle-of-attack history. By previous angle-of-attack history, we refer to both dynamic angle-of-attack changes due to body motion as well as to the downwash history due to three-dimensional effects. If the angle-of-attack history is known, the unsteady lift may be found using a functional form first presented by Jones,[15] who extended Theodorsen's[16] oscillating flat-plate airfoil results to arbitrary motions. The functional form of the lift equation is given by

$$\begin{aligned} C_l(s) = {} & \pi\left(\frac{c}{2V_\infty^2}\ddot{h} + \frac{c}{2V_\infty}\dot{\alpha} - \frac{c^2 a}{4V_\infty^2}\ddot{\alpha}\right) \\ & + 2\pi\left[\frac{\dot{h}(0)}{V_\infty} + \alpha(0) + \frac{c}{2V_\infty}\left(\frac{1}{2} - a\right)\dot{\alpha}(0)\right]\phi(s) \\ & + 2\pi\int_0^s \left[\frac{c}{2V_\infty^2}\ddot{h} + \frac{c}{2V_\infty}\dot{\alpha}\right. \\ & \left. + \frac{c^2}{4V_\infty^2}\left(\frac{1}{2} - a\right)\ddot{\alpha}\right]\phi(s - \sigma)\,d\sigma \end{aligned} \tag{2}$$

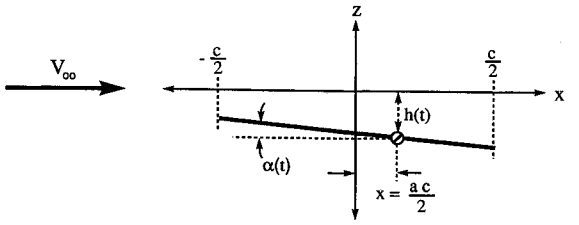

Fig. 4 Nomenclature for Eq. (2).

where c is the chord length, s $(=2V_\infty t/c)$ is the half-chord nondimensional time, a is the pitch/plunge location (a is -1 for the leading edge and $+1$ for the trailing edge), an overdot represents a derivative with respect to time, and $\phi(s)$ is the Wagner function[17] given by Ref. 5

$$\phi(s) = \frac{s+2}{s+4} \tag{3}$$

The nomenclature for Eq. (2) is provided in Fig. 4, with pitch location $ac/2$, vertical displacement $h(t)$, and angle of attack $\alpha(t)$ positive as shown.

Equation (2) is informative as it reveals the nature of both noncirculatory and circulatory lift terms. The noncirculatory terms are the first three terms in Eq. (2) and exist as long as the airfoil is in motion. The noncirculatory terms are associated with satisfying the "no-flow" boundary condition on the surface of the airfoil. The circulatory terms are the ones involving the Wagner function $\phi(s)$, and require a convection time before they attain their full magnitude, as they are associated with the shedding of vorticity into the wake. This distinction between the noncirculatory and the circulatory terms will be used later when we derive a formulation for the unsteady bound circulation. Equation (2) has been tested for various pitch motions by way of a two-dimensional unsteady paneling code, and the equation was found to predict the unsteady lift well.[13,14] Equation (2) can be modified to reflect airfoils other than flat-plate airfoils by way of the 2π multiplier in both of the circulatory terms. The value of 2π is the steady, lift-curve slope which can be altered to reflect thick airfoils, thereby resulting in better agreement with unsteady two-dimensional paneling codes.[13,14] The two-dimensional unsteady paneling code employed in these tests was based on the method developed by Basu and Hancock.[18] The method of Basu and Hancock is unique in that their unsteady Kutta-condition formulation involved a flexible trailing-edge wake panel, thereby ensuring a zero unsteady pressure gradient across the wake. Supportive results of the Basu and Hancock method were presented by Poling and Telionis[19] in their experimental investigation of oscillating (in pitch) airfoils.

The form of Eq. (2) enables the calculation of unsteady lift due to a dynamic body motion; however, the lift (or loss of lift) caused by downwash effects must still be treated. The unsteady lift due to a time varying downwash may be found by considering it as being identical to a plunging motion. Therefore, the lift due to downwash may be written as follows:

$$C_l^{\text{dw}} = -\pi \frac{c\dot{w}}{2V_\infty^2} - 2\pi \frac{w(0)}{V_\infty} \phi(s) - 2\pi \int_0^s \frac{c\dot{w}}{2V_\infty^2} \phi(s-\sigma)\, d\sigma \tag{4}$$

with the sign convention as in Fig. 4, a time-invariant downwash is thus equivalent to a motion where the airfoil plunges upwards ($\dot{h}$ is negative and constant). The downwash is represented by w and taken to be positive if downward with respect to the airfoil; thus the following relations exist between w and vertical displacement h:

$$w = -\dot{h} \tag{5a}$$

$$\dot{w} = -\ddot{h} \tag{5b}$$

Provided that the downwash and body motion histories are known, the total lift may be evaluated by way of Eqs. (2) and (4).

B. Unsteady Moment Relation

As in the case of the unsteady lift, the unsteady moment is also calculated using a method similar to Jones' extension of Theodorsen's oscillating flat-plate airfoil results to arbitrary motions[15] (cf., unsteady lift relation, discussed previously). The functional form of the moment equation is given by

$$C_{m_y}(s) = \pi \left[\frac{ca}{4V_\infty^2} \ddot{h} - \frac{c(\frac{1}{2}-a)}{4V_\infty} \dot{\alpha} - \frac{c^2(\frac{1}{8}+a^2)}{8V_\infty^2} \ddot{\alpha} \right] + \frac{\pi}{2} \left[\frac{2E}{V_\infty} \dot{h}(0) + 2E\alpha(0) + \frac{cE(\frac{1}{2}-a)}{V_\infty} \dot{\alpha}(0) \right] \phi(s) + \frac{\pi}{2} \int_0^s \left[\frac{Ec}{V_\infty^2} \ddot{h} + \frac{Ec}{V_\infty} \dot{\alpha} + \frac{c^2E(\frac{1}{2}-a)}{2V_\infty^2} \ddot{\alpha} \right] \phi(s-\sigma)\, d\sigma \tag{6}$$

where

$$E = (\tfrac{1}{2} + a)$$

The moment in Eq. (6) is summed about the pitch location $x = a$. Equation (6) may also be modified to reflect airfoils other than flat-plate airfoils by way of the $(\pi/2)$ multiplier in both of the circulatory terms, as has been previously mentioned for Eq. (2). The moment in Eq. (6) is the unsteady moment due to body motions; however, the unsteady moment due to downwash effects has yet to be considered. This unsteady moment due to downwash effects is taken to be identical to a plunging motion, thus using the convention of Eqs. (5a) and (5b), the unsteady moment coefficient due to downwash is given by

$$C_{m_y}^{\text{dw}}(s) = -\pi \frac{ca\dot{w}}{4V_\infty^2} - \pi \frac{(\frac{1}{2}+a)w(0)}{V_\infty} \phi(s) - \frac{\pi}{2} \int_0^s \left[\frac{(\frac{1}{2}+a)c}{V_\infty^2} \dot{w} \right] \phi(s-\sigma)\, d\sigma \tag{7}$$

Through the knowledge of the downwash and body motion histories, the total lift is evaluated by Eqs. (2) and (4), and the total moment by Eqs. (6) and (7). Before the downwash can be calculated, however, the vortex strengths (bound and wake) must be known.

C. Unsteady Circulation Relation

In order to derive a relation between the circulation and angle-of-attack history, recall the previous discussion on noncirculatory and circulatory lift. We shall assume that the bound circulation is created in the same functional manner as the circulatory lift, thus adopting the form of Eq. (2) we write ($V_\infty = c = 1$ for the present case)

$$\Gamma(s) = [2c_1\dot{h}(0) + 2c_2\alpha(0) + 2c_3\dot{\alpha}(0)]\phi^{\text{circ}}(s) + \int_0^s (c_1\ddot{h} + c_2\dot{\alpha} + c_3\ddot{a})\phi^{\text{circ}}(s-\sigma)\, d\sigma \tag{8}$$

where c_1, c_2, and c_3 are yet to be determined constants and ϕ^{circ} is a circulation buildup function, also yet to be determined. By comparing Eqs. (2) and (8), it is noticed that c_1 and c_2 are equal to each other (for $V_\infty = 1$), leaving only two constants and ϕ^{circ} to be determined. The form of ϕ^{circ} was determined by obtaining the circulation buildup for a Wagner-type indicial problem using either Wagner's result directly (Ref. 17), or the unsteady two-dimensional paneling code[18]

and fitting a function to the buildup curve. A representative function was found to be

$$\phi^{\text{circ}}(s) = \frac{s^2 + s}{0.975s^2 + 3.4s + 1.6} \tag{9}$$

where s is once again the half-chord nondimensional time. Figure 5 shows a comparison of the buildup in nondimensional circulation predicted by Eq. (9) to that given by Wagner or alternatively predicted by the two-dimensional paneling code; all are virtually identical.

The values of constants c_1 and c_3 are dependent on the type of airfoil section being investigated, and it can also be assumed from Eq. (2) that c_3 is a function of pitch location. The value of c_1 may be determined using the two-dimensional unsteady paneling code by executing a constant-$\dot{\alpha}$ pitch motion with the pitch axis at the three-quarter-chord location. This pitch axis location was chosen to ensure that $a = \frac{1}{2}$ [cf., Eq. (2)], thus "turning off" any circulation production associated with the c_3 term. The value of c_3 may then be solved for using the two-dimensional unsteady paneling code and Eq. (8) for an oscillating angle-of-attack motion.

The circulation relation presented in Eq. (8) is for body motions only. A formulation relating the unsteady circulation buildup to the downwash may be found by introducing Eqs. (5a) and (5b) into Eq. (8), resulting in

$$\Gamma^{\text{dw}} = -2c_1 w(0)\phi^{\text{circ}}(s) - \int_0^s c_1 \dot{w}\phi^{\text{circ}}(s - \sigma)\, d\sigma \tag{10}$$

Thus, by using Eqs. (8) and (10) to solve for the strengths of the bound circulation and wake vortices, and by using Eqs. (2) and (4) to solve for the lift, and Eqs. (6) and (7) to solve for the moment, the unsteady wing loading can be determined for any pitch/plunge-type motion.

D. Numerical Implementation

The numerical implementation of the unsteady lifting-line technique is achieved by breaking the wing (bound vortex) up into discrete segments, each of which possesses that particular segments two-dimensional unsteady airfoil characteristics. The spanwise vortices being shed into the wake at a particular segment are solved for by the difference in bound circulation between the present and the previous time step, therefore, at any y location

$$\Gamma^{\text{span}}(y) = -[\Gamma(y, t) - \Gamma(y, t - \Delta t) + \Gamma^{\text{dw}}(y, t) - \Gamma^{dw}(y, t - \Delta t)] \tag{11}$$

The shed spanwise vortex of strength $\Gamma^{\text{span}}(y)$ from Eq. (11) is placed $V_\infty \Delta t$ downstream of the bound vortex. The streamwise vortices are shed between each of the spanwise discrete segments and are equal in strength to the difference between the inward (i.e., $y - \Delta y$ for the $+y$ side of the wing) segments

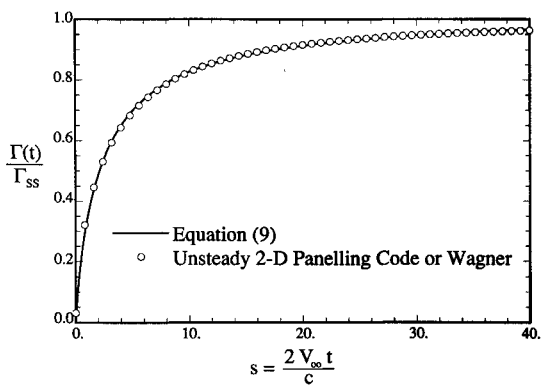

Fig. 5 Circulation buildup function ϕ^{circ}.

bound circulation and the current (y) segments bound circulation. Thus, the strength of these streamwise vortices connecting the bound and shed spanwise vortices may be written as

$$\Gamma^{\text{stream}}(y) = \Gamma(y - \Delta y, t) + \Gamma^{\text{dw}}(y - \Delta y, t) - \Gamma(y, t) - \Gamma^{\text{dw}}(y, t) \tag{12}$$

The length of this streamwise vortex is equal to $V_\infty \Delta t$.

The numerical implementation begins at $t = \Delta t$, where the first body motion is allowed to take place. The bound circulation is then solved for using Eq. (8), and the spanwise and streamwise vortices are allowed to convect $V_\infty \Delta t$ downstream of the bound vortex. The downwash is then evaluated at the midpoint of each bound vortex segment. The bound circulation due to the downwash is then calculated using Eq. (10) and summed with the bound circulation [from Eq. (8)] due to the body motion in the second time step. The wake vortices from the first time step are then allowed to convect another $V_\infty \Delta t$, while the current bound circulation is used with Eqs. (11) and (12) to determine the strength of the wake vortices $V_\infty \Delta t$ downstream of the bound vortex. The downwash is once again evaluated and the cycle repeated. One subtle but very important point with regard to the downwash calculation must be emphasized; the spanwise vortices directly downstream of any y segment have already been incorporated into Eqs. (8) and (10) through the two-dimensional theory. Thus, only the difference in vortex strength between any specific downstream spanwise vortex and that due to another segment ($y + \Delta y$ for example) should be included in the downwash calculation. The spanwise lift is evaluated at each time step using Eqs. (2), (4), (5a), and (5b), and the spanwise moment is evaluated at each time step using Eqs. (6) and (7). Since the wake vortices were assumed to convect at V_∞, the wake is planar.

It may not be immediately obvious why we constructed our lifting-line model the way that we did, so some explanation follows. The inclusion of all streamwise vortices in the computation of the downwash at a particular wing location follows directly from steady lifting-line theory. The inclusion of only the difference in the strength of the spanwise free vortices from that associated with the particular span location (at which the downwash was being computed) was based on the meaning of the shed and bound vortex pairs in two-dimensional theory. In two-dimensional flow, the strength of the vortex pairs (i.e., shed and bound) are such that the flow does not penetrate the surface of the airfoil; thus, there is no "downwash" associated with the shed free vortex. Furthermore, in two-dimensional flow, the vortices are assumed to extend in and out of the section plane to infinity. Thus, at a particular span location on a wing, the only free, spanwise vortices that contribute to downwash would be those which are different from the free vortex shed by the wing spanwise section of interest at the same streamwise location.

The decision to place the starting spanwise vortex at a distance $V_\infty \Delta t$ from the bound wing vortex was not an easy decision, but was made for identical reasons to those discussed in Ref. 7. The determining factor was the fact that the wing must be considered as a vortex filament with no chord dimension.

IV. Comparisons

The ideas contained in the theory section were implemented in a Fortran 77 code and run on both a NeXTstation computer and a Sun SPARC station 1. In this section the results of rectangular wings of various aspect ratios and wing-section types performing an angle-of-attack jump from 0 to 5 deg are compared with the results for the same wing geometries from two codes. The first code was a constant-source, constant-doublet method, PMARC,[20] which we ran on the Sun. The second code was a vortex-lattice method for which the results

of the Wagner indicial motion for rectangular, flat-plate wings of various aspect ratios are given in Katz and Plotkin.[21]

A. Wing Loading

Figures 6 and 7 show lift buildup as a function of half-chord nondimensional time s for various aspect ratios as predicted by the unsteady lifting-line theory, the vortex-lattice method (Fig. 6), and by PMARC (Fig. 7). In both comparisons the agreement is quite good. It should be noted that the results of Fig. 6 are for a flat-plate wing, while those of Fig. 7 are for a NACA 0012. Figures 6 and 7 show only the integrated lift, a more detailed inspection of the capabilities of the unsteady lifting-line method can be seen by examining the time history of the downwash and span loading. Figure 8 shows the downwash as a function of nondimensional time; also given in the figure is the downwash predicted for the same wing geometry by steady lifting-line theory. Several points may be made here; the downwash initially is essentially zero over the span except for right at the wingtips. One can conclude that the lift is essentially two-dimensional-like up to a nondimensional time of 0.01. After a nondimensional time of 0.1 the downwash has relaxed a bit. By a nondimensional time of 0.5, the downwash is nearly that for the steady three-dimensional case. Figure 9 shows the concomitant lift distribution. The final point is that the lift distribution approaches that predicted by steady lifting-line theory, a requirement of the method.

Figure 10 compares the wing loading predicted by the unsteady lifting-line method for an aspect ratio of 8 (AR = 8) rectangular wing of NACA 0012 section with that predicted by PMARC. Cross reference to Fig. 7 shows that the integrated lift for AR = 8 is nearly the same for both the unsteady lifting-line method and PMARC after a time $s \simeq 1.0$, which would correspond to a $t^* = 0.0625$. While the integrated lift is nearly the same, the detailed span loading is not the same until $t^* \geq 0.5$, which corresponds to a $s = 8$. Detailed inspection of Fig. 10 shows that PMARC predicts an elevated tip loading above that of further inboard locations. This elevated tip loading makes up for the otherwise lower inboard loading predicted by PMARC, and explains why the integrated lifts are nearly the same for s smaller than 8. A further

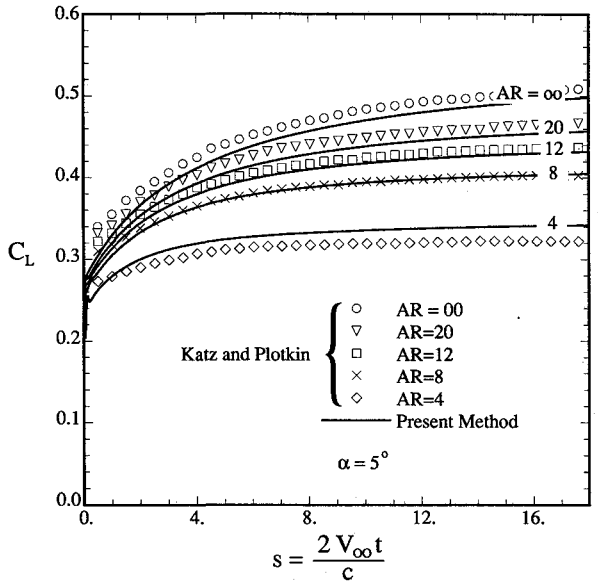

Fig. 6 Comparison of the total wing transient lift on a flat-plate wing between the present method and that by Katz and Plotkin[21] for the indicial problem.

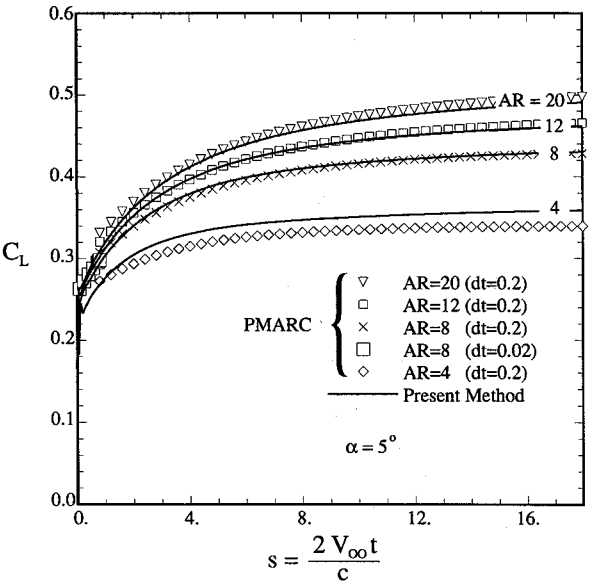

Fig. 7 Comparison of the total wing transient lift on a rectangular NACA 0012-section wing between the present method and PMARC for the indicial problem.

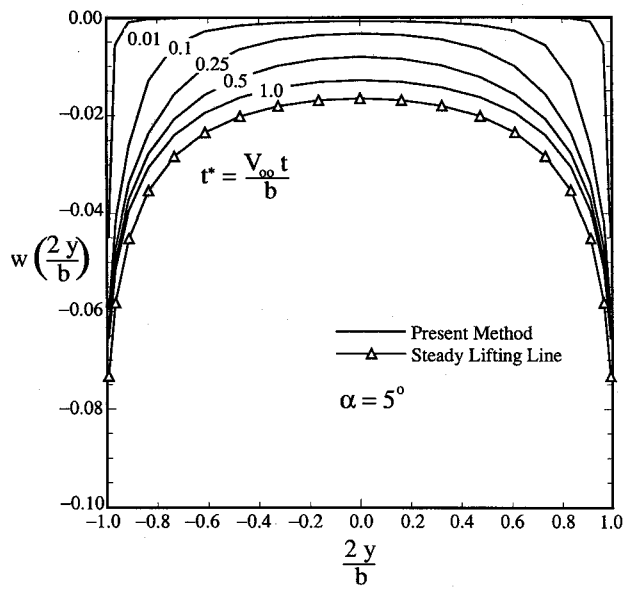

Fig. 8 Transient downwash for the indicial problem on an AR 6 rectangular wing with a NACA 0012 section also giving the steady lifting-line prediction.

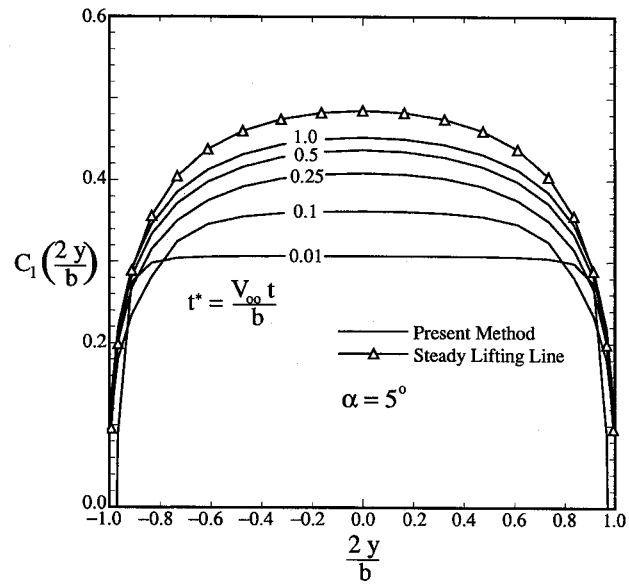

Fig. 9 Transient lift for the indicial problem on an AR 6 rectangular wing with a NACA 0012 section.

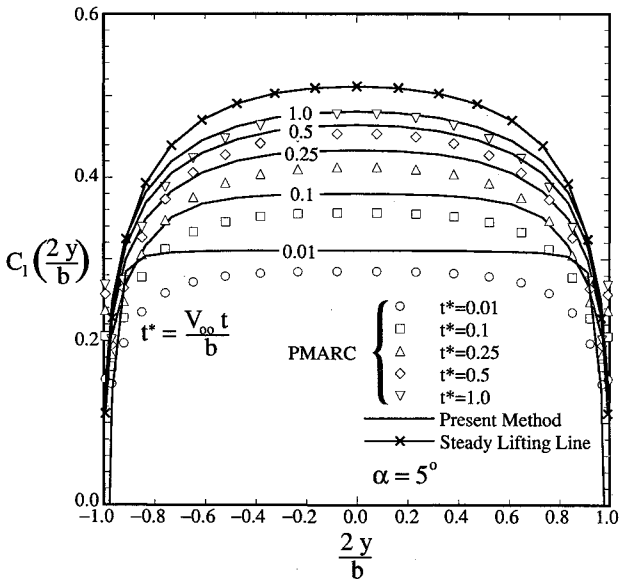

Fig. 10 Transient lift for the indicial problem on an AR 6 rectangular wing with a NACA 0012 section present method and PMARC.

note can be made with regard to the lift predicted by the vortex-lattice method and PMARC in Figs. 6 and 7 in that the lift values are not shown for times earlier than $s = 0.08$. The reason for not showing these early lift values is that they are so large that they are off the scale of the figure. This behavior is attributable to the noncirculatory lift (sometimes referred to as apparent-mass spike) found at the beginning of all indicial motion response functions. The length of time that the noncirculatory lift affects the total lift buildup is, however, dependent upon the time-step size. For example, in Fig. 7 the time step was 0.2 and the first few points are above that predicted by the unsteady lifting-line theory. The additional points for AR = 8 in Fig. 7 are for a $\Delta t = 0.02$ (the curve for PMARC in Fig. 10 for $t^* = 0.01$ was obtained using this time step). This means that the early-time predictions for PMARC are time-step dependent, as will be the vortex-lattice method since it exhibits similar tendencies. This solution dependence upon time-step size can have a large effect on the program run time, as described in the following.

B. Run Times

The unsteady lifting-line code was run on both a NeXTstation and a Sun SPARC station 1; both machines gave comparable run times, so that all further comparisons are based on Sun run times only. Consider the results of Fig. 7; here the results for PMARC were also obtained on the Sun. The runs to $s = 18.0$ took approximately 2.5 h for PMARC and approximately 15 min for the unsteady lifting-line method. The runs for the unsteady lifting-line method were for a $\Delta t = 0.01$. The PMARC runs were for a time step of 0.2; however, for a time step of 0.02 PMARC took approximately 48 h to get to a s of only 9.6 for AR = 8. In fact, because of the early time-step problems associated with paneling methods discussed earlier, the 48-h comparison is probably more appropriate. This is because any arbitrary motions need to be highly resolved and require prior history information developed at the same time step.

C. Arbitrary Motions and Dynamic Camber Change

The unsteady lifting-line method has more advantages than just run times. In the previous section we mentioned that the 48-h comparison was more realistic when considering arbitrary motions; in fact, PMARC is not able to handle arbitrary dynamic wing motions. As described in the documentation for PMARC, dynamic motions are specifically limited to an indicial motion and constant-rate rotational (pitch, roll, and yaw) motions. These restrictions appear to be due to the way in which the source/sink panels are computed. Changing the code architecture to accommodate arbitrary, moving boundary conditions would appear to increase run times significantly. Furthermore, dynamic camber changes (i.e., flap motions) appear to be even more prohibitive. On the other hand, the unsteady lifting-line method has no such restrictions on motion, and with only minor changes could accommodate dynamic camber motions.[13,14]

V. RWW Experiment

Finally, we examine the RWW data[2]; Fig. 11 gives one of the data sets of coefficient of lift vs nondimensional time at various span locations, for near constant angular-rate motions about the quarter-chord position,[2] with the nondimensional pitch rate defined as

$$\dot{\alpha}^+ = (\dot{\alpha}c/V_\infty) \tag{13}$$

These tests were conducted in a 3-ft by 3-ft tunnel with a rectangular wing of section NACA 0015, semispan 1 ft and chord 0.5 ft. An observation was made that these data appear more two-dimensional-like than three-dimensional-like, in that the C_l curves at each span location are closer together than one would expect if the lift were distributed in a steady three-dimensional form. Of interest to this article is the portion of the curves that can be considered "attached flow"; for our purpose we will consider the data up to approximately 25 deg. Before comparing the unsteady lifting-line predictions to the RWW data, consider first a comparison of the unsteady lifting-line predictions to that for steady lifting-line theory, both for a wing of the RWW geometry. Figure 12 gives this comparison of C_l vs nondimensional time curves at the same span locations, and it can be seen that the curves are markedly different. It should be mentioned that in producing the unsteady lifting-line results for this section, an experimental lift curve slope of 6.0 was used instead of the flat-plate airfoil value of 2π in Eq. (2).

These differences, however, make good physical sense. As pointed out in Ref. 22, an abrupt constant-pitch-rate motion

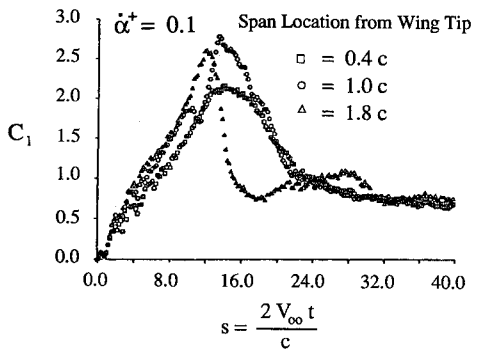

Fig. 11 RWW Sectional lift data vs nondimensional time for $\dot{\alpha}^+ = 0.1$ (Ref. 2, by permission).

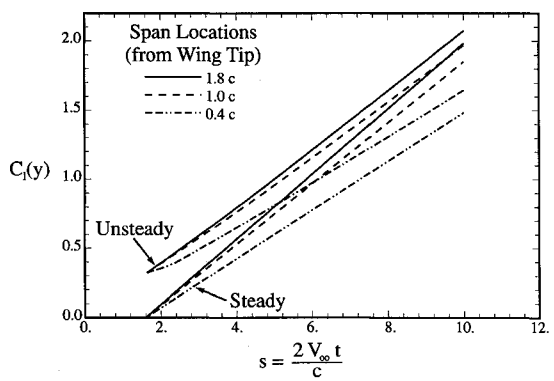

Fig. 12 Steady vs unsteady lifting-line prediction of section lift coefficient for $\dot{\alpha}^+ = 0.1$.

in two-dimensional flow produces a sudden jump in C_l and a concomitant lift-curve slope depression. These effects have been experimentally demonstrated.[22] The sudden jump in C_l is attributable to noncirculatory effects and exhibits itself immediately upon motion onset. The slope depression, on the other hand, is due to circulatory effects which require time to fully develop, a two-dimensional effect. The slope is further depressed by the developing three-dimensional wake, as in steady flow; therefore, the slope nearest the wingtip is depressed more than those inboard.

Figure 13 compares the unsteady lifting-line prediction to the RWW data. In performing this comparison, the motion history for the unsteady lifting-line prediction was an idealized ramp motion. The experimental motion history, being a real ramp motion, was found to begin at $s \approx 1$ and attain a constant pitch rate by a half-chord nondimensional time of $s \approx 2$. In order to account for the differences between the idealized and real ramp motions, the onset of motion for the unsteady lifting-line method was postponed until a half-chord nondimensional time of $s = 1.6$. The angle of attack for the simulation using the lifting-line theory can be calculated from the half-chord nondimensional time (s) by means of the following equation:

$$\alpha = 2.87(s - 1.6) \tag{14}$$

where α is in degrees. It is clear from Fig. 13 that most of the "two-dimensional-like" character of the data can be attributed to the noncirculatory lift jump. The similarity to the data is quite good and certainly matches the overall characteristics, not to mention the quantitative nature of the data. These results (Fig. 13) lend further credibility to the unsteady lifting-line method, but they do more. It is now possible to understand in more detail why the results of the RWW experiment turned out the way that they did.

Figure 14 shows the load distribution predicted by the unsteady lifting-line theory as a function of half-chord nondimensional time and instantaneous angle of attack, along with a steady lifting-line prediction for the same angle of attack. At $\alpha = 0.3$ deg the noncirculatory C_l jump accounts for virtually all of the lift. As time increases, two effects combine to reduce the difference between the steady and unsteady predictions. First, the growing wake begins to reduce the effective angle of attack to varying degrees depending on the span location; but additionally, the large noncirculatory lift contribution that continues to be in effect as long as the motion persists is being overrun by the reduced buildup of circulatory lift over that which would be present in steady flow at that angle of attack. By an angle of attack of 15 deg the two competing effects are causing the steady and unsteady loads to draw even closer together; but it should be noted that the steady lift is still *less* than the unsteady lift.

The fact that the unsteady lift is greater than that of the wing at the same angle of attack in steady flow even at 15-deg angle of attack, is of interest. Reasoning that unsteady

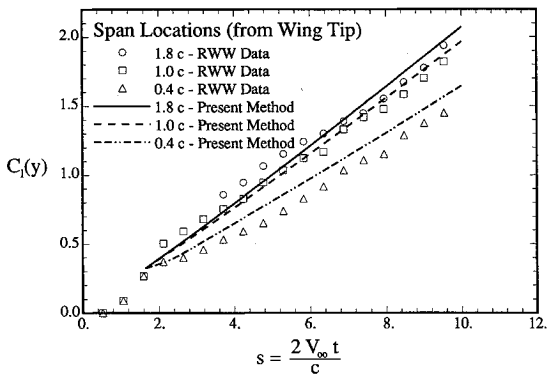

Fig. 13 Comparison of the present method section lift coefficient with RWW data for $\dot{\alpha}^+ = 0.1$.

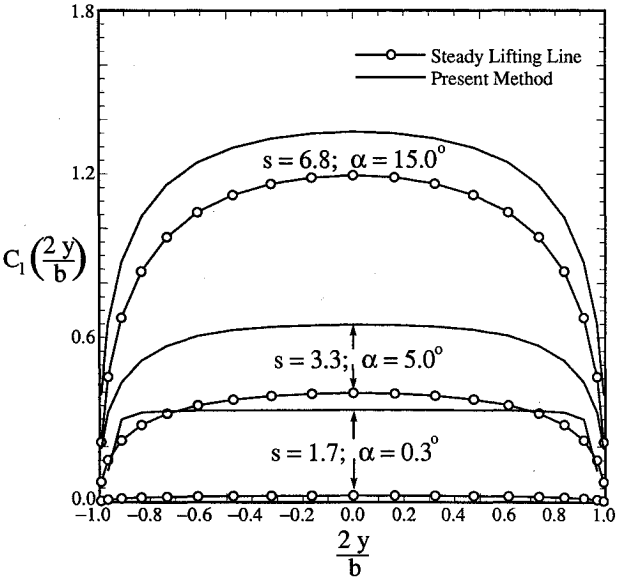

Fig. 14 Predicted spanwise lift during $\dot{\alpha}^+ = 0.1$ pitch motion.

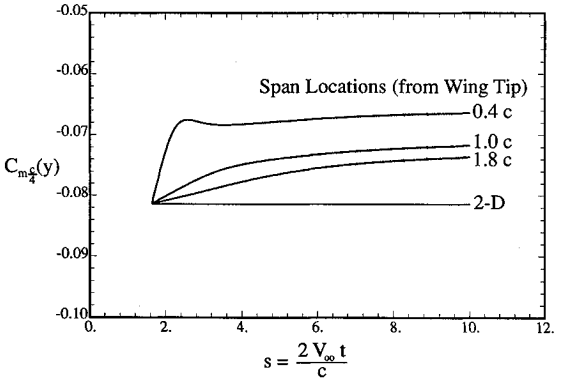

Fig. 15 Comparison of the present method section moment coefficient with Eq. (15) for $\dot{\alpha}^+ = 0.1$.

lift lags behind steady lift (developed from concepts of indicial motions) could lead to some design surprises. In fact, at high angular rates the noncirculatory terms are significant, and as demonstrated in Fig. 14, dominate the load over much of the motion history. Finally, the results of Fig. 13 should be viewed as a second and conclusive experimental demonstration of the lift character of pitching motions as described in Ref. 22.

As mentioned previously, the unsteady lifting-line technique is also capable of predicting unsteady spanwise moments. For the case of the RWW experiment, two-dimensional unsteady theory predicts the unsteady quarter-chord moment by means of Eq. (6) as

$$C_{m_{(c/4)}} = -(\pi/4)\dot{\alpha}^+ \tag{15}$$

Thus, the unsteady quarter-chord moment for a constant pitch rate motion about the quarter chord is a constant value in two-dimensional theory. The quarter-chord moment predicted by the present method as well as by two-dimensional unsteady theory [Eq. (15)] is shown in Fig. 15 for the case of the RWW experiment. Reconsidering Eqs. (6) and (7) for the case of a constant pitch rate motion about the quarter chord ($a = -\frac{1}{2}$), the quarter-chord moment can be rewritten as

$$C_{m_{(c/4)}}(s) = -\frac{\pi c}{4V_\infty}\dot{\alpha} + \frac{\pi c}{8V_\infty^2}\dot{w} \tag{16}$$

Equation (16) shows that the two-dimensional moment effect given by Eq. (15) is present in Eq. (16) (first term, right side),

and remains the same for all span locations; however, the moment becomes spanwise-dependent due to the time rate of change of the downwash $\dot{w}$, which in general, is spanwise-dependent. Applying this knowledge to the interpretation of Fig. 15, it is seen that for early times ($s < 3$) the time rate of change of downwash is greatest at the wingtip. The quarter-chord moment is then seen to level off to a constant but span location-dependent value, consistent with the fact that the magnitude of the time rate of change in downwash decreases with distance from the wingtip.

VI. Conclusions

This article presented the development and verification of an unsteady lifting-line method that is both quick and versatile. The resulting agreement between the present method and that of existing numerical codes, as well as the agreement with experimental data suggests that the most essential physics of the unsteady wing loading are being modeled correctly. Whether it can be argued that the more complex methods of modeling unsteady three-dimensional wing loading are more accurate or not, or whether these more complex methods can be made to accommodate arbitrary motions and camber change, the fact remains that these methods cannot be made to be quick. As such, application of complex unsteady aerodynamic methods to interactive problems in controls, aeroelasticity, etc., requires quantum improvements in computing machines. On the other hand, the unsteady lifting-line method presented here can handle arbitrary wing motions, nonsymmetric loading, and can be easily extended to handle unsteady camber/flap changes with no increase in computational run times. The present computational run times on desktop-type workstations are appropriate for interactive problems in the areas of controls and aeroelasticity. Although run-time and supercomputer availability may be of increasingly less concern, this simple unsteady lifting-line method offers a useful contribution to applied aerodynamics.

Acknowledgments

This work was supported by a research contract from the McDonnell Douglas Corporation, under the technical management of Richard E. Boalbey. We are appreciative for not only the financial support but also the technical support and suggestions of both Boalbey and Wayne Ely of McDonnell.

References

[1]Kuethe, A. M., and Chow, C. Y., *Foundations of Aerodynamics: Bases of Aerodynamic Design, Third Edition*, Wiley, New York, 1976.

[2]Robinson, M., Wissler, J., and Walker, J., "Unsteady Surface Pressure Measurements on a Pitching Rectangular Wing," AIAA Paper 88-0328, Jan. 1988.

[3]Jumper, E. J., Dardis, W. J., III, and Stephen, E. J., "Toward an Unsteady-Flow Airplane," AIAA Paper 88-0752, Jan. 1988.

[4]Lang, J. D., and Francis, M. S., "Unsteady Aerodynamics and Dynamic Aircraft Maneuverability," *Proceedings of the AGARD Symposium on Unsteady Aerodynamics—Fundamentals and Applications to Aircraft Dynamics*, Göttingen, Germany, May 1985, pp. 29:1–19.

[5]Bisplinghoff, R. L., Ashley, H., and Halfman, R. L., *Aeroelasticity*, Addison-Wesley, Reading, MA, 1955.

[6]Cicala, P., "Comparison of Theory with Experiment in the Phenomenon of Wing Flutter," NACA TM 887, 1939.

[7]Dengler, M. A., and Goland, M., "The Calculations of Spanwise Loadings for Oscillating Airfoils by Lifting Line Techniques," *Journal of the Aeronautical Sciences*, Vol. 19, No. 11, 1952, pp. 751–759.

[8]Fung, Y. M., *An Introduction to the Theory of Aeroelasticity*, Dover, New York, 1969.

[9]Beddoes, T. S., "Two and Three Dimensional Indicial Methods for Rotor Dynamic Airloads," American Helicopter Society/National Specialist's Meeting on Rotorcraft Dynamics, Arlington, TX, Nov. 1989.

[10]Jumper, E. J., and Hugo, R. J., "Simple Theories of Dynamic Stall that are Helpful in Interpreting Computational Results," *Computer Physics Communications*, Vol. 65, 1991, pp. 158–163.

[11]Prandtl, L., and Tietjens, O. G., *Applied Hydro- and Aeromechanics*, Dover, New York, 1934.

[12]Milne-Thomson, L. M., *Theoretical Aerodynamics*, 4th ed., Dover, New York, 1958.

[13]Hugo, R. J., "The Aerodynamic Characteristics of Airfoils Undergoing Rapid Angle of Attack and Camber Changes," M.S. Thesis, Univ. of Notre Dame, Notre Dame, IN, 1991.

[14]Hugo, R. J., and Jumper, E. J., "Controlling Unsteady Lift Using Unsteady Trailing-Edge Flap Motions," AIAA Paper 92-0275, Jan. 1992.

[15]Jones, W. P., "Aerodynamic Forces on Wings in Non-Uniform Motion," British Aeronautical Research Council, R&M 2117, London, 1945.

[16]Theodorsen, T., "General Theory of Aerodynamic Instability and the Mechanism of Flutter," NACA TR 496, 1935.

[17]Wagner, H., "Über die Entstehung des dynamischer Auftrebes von Tragflügeln," *Zeitschrift fuer Angewandte Mathematik und Mechanik*, Vol. 5, No. 1, 1925, pp. 17–35.

[18]Basu, B. C., and Hancock, G. J., "The Unsteady Motion of a Two-Dimensional Airfoil in Incompressible Inviscid Flow," *Journal of Fluid Mechanics*, Vol. 87, No. 1, 1978, pp. 159–178.

[19]Poling, D. R., and Telionis, D. P., "The Response of Airfoils to Periodic Disturbances—The Unsteady Kutta Condition," *AIAA Journal*, Vol. 24, No. 2, 1986, pp. 193–199.

[20]Ashby, D. L., Dudley, M. R., and Iguchi, S. K., "Development and Validation of an Advanced Low-Order Panel Method," NASA TM 101024, Oct. 1988.

[21]Katz, J., and Plotkin, A., *Low-Speed Aerodynamics from Wing Theory to Panel Methods*, McGraw-Hill, New York, 1991.

[22]Jumper, E. J., Schreck, S. J., and Dimmick, R. L., "Lift-Curve Characteristics for an Airfoil Pitching at Constant Rate," *Journal of Aircraft*, Vol. 25, No. 10, 1987, pp. 680–687.